Fig. S1

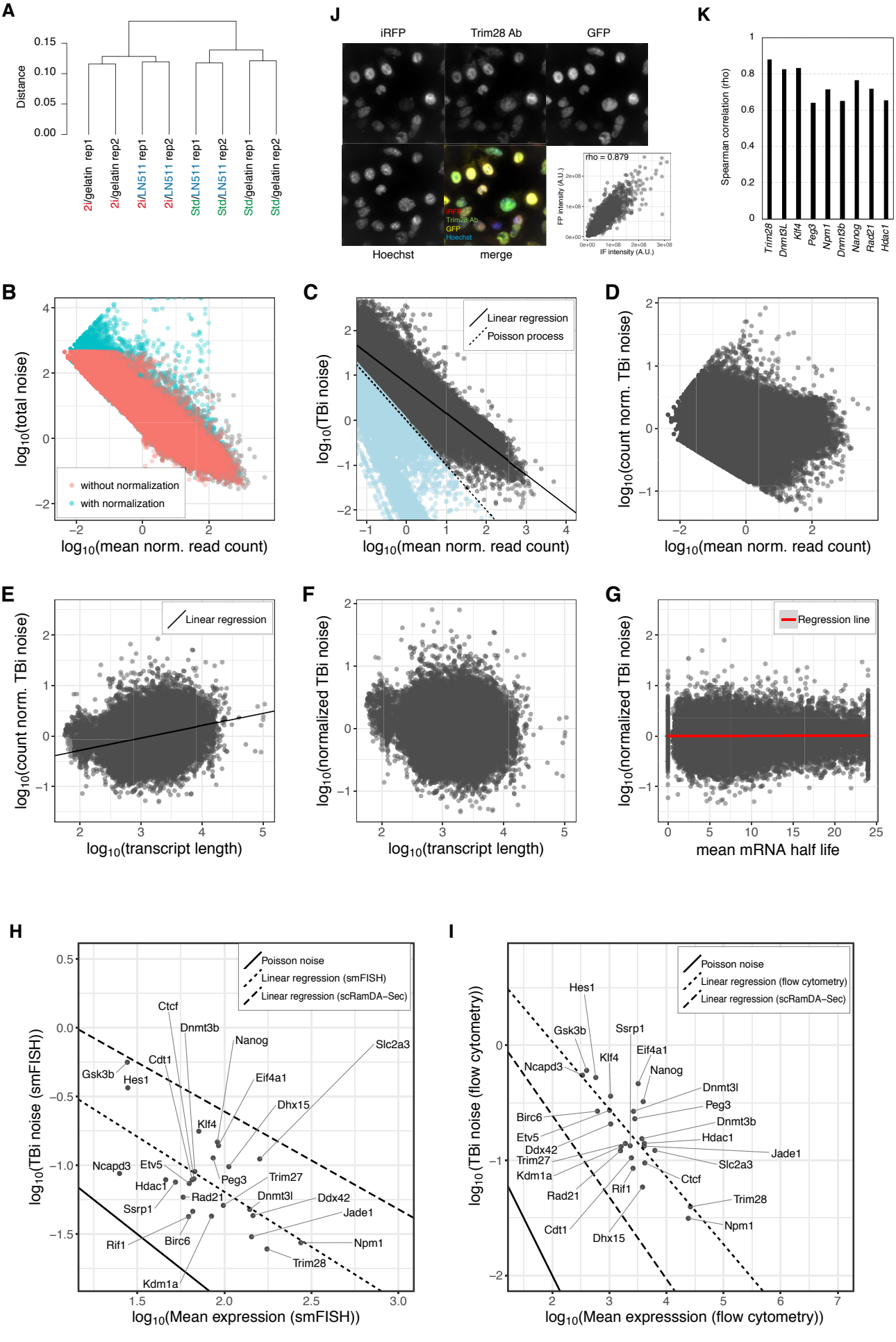
A
Distance
0.15
0.10
0.05
0.00
2i/gelatin rep1
2i/gelatin rep2
2i/LN511 rep1
2i/LN511 rep2
Std/LN511 rep1
Std/LN511 rep2
Std/gelatin rep1
Std/gelatin rep2
J
iRFP
Trim28 Ab
GFP
Hoechst
merge
rho = 0.879
FP intensity (A.U.)
IF intensity (A.U.)
K
Spearman correlation (rho)
Trim28
Dnmt3L
Klf4
Peg3
Npm1
Dnmt3b
Nanog
Rad21
Hdac1
B
log10(total noise)
without normalization
with normalization
log10(mean norm. read count)
C
Linear regression
Poisson process
log10(TBi noise)
log10(mean norm. read count)
D
log10(count norm. TBi noise)
log10(mean norm. read count)
E
Linear regression
log10(count norm. TBi noise)
log10(transcript length)
F
log10(normalized TBi noise)
log10(transcript length)
G
Regression line
log10(normalized TBi noise)
mean mRNA half life
H
Poisson noise
Linear regression (smFISH)
Linear regression (scRamDA–Sec)
log10(TBi noise (smFISH))
log10(Mean expression (smFISH))
Ctcf
Dnmt3b
Nanog
Slc2a3
Cdt1
Gsk3b
Hes1
Eif4a1
Dhx15
Klf4
Ncapd3
Etv5
Peg3
Trim27
Hdac1
Rad21
Dnmt3l
Ddx42
Ssrp1
Jade1
Rif1
Birc6
Npm1
Trim28
Kdm1a
I
Poisson noise
Linear regression (flow cytometry)
Linear regression (scRamDA–Sec)
log10(TBi noise (flow cytometry))
log10(Mean expresssion (flow cytometry))
Hes1
Gsk3b
Ssrp1
Eif4a1
Klf4
Ncapd3
Nanog
Dnmt3l
Peg3
Birc6
Dnmt3b
Etv5
Hdac1
Ddx42
Jade1
Trim27
Slc2a3
Kdm1a
Ctcf
Rad21
Rif1
Trim28
Cdt1
Dhx15
Npm1

Fig. S2

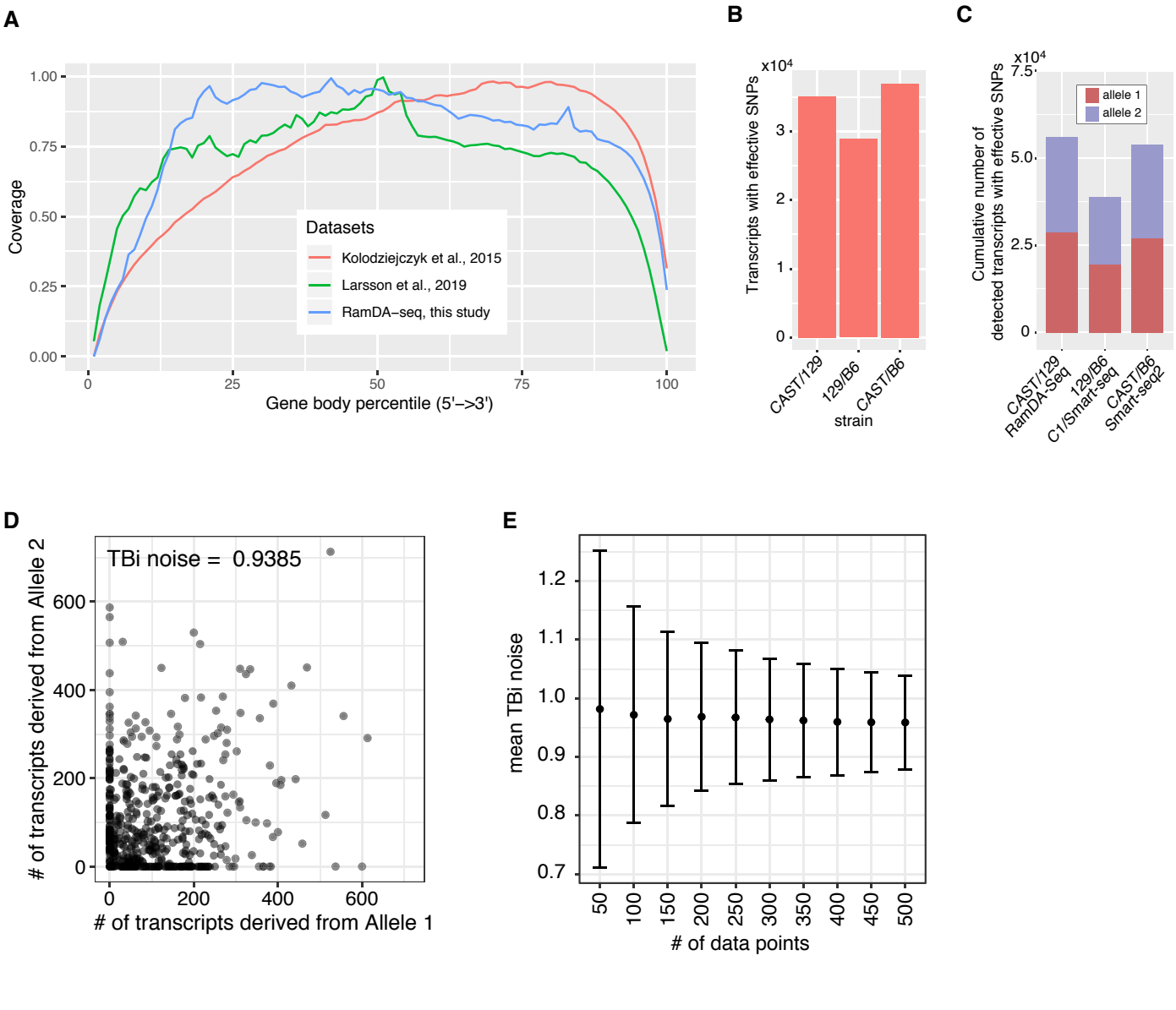
A
Coverage
Gene body percentile (5'–>3')
Datasets
Kolodziejczyk et al., 2015
Larsson et al., 2019
RamDA–seq, this study
B
Transcripts with effective SNPs
x10^4
CAST/129
129/B6
CAST/B6
strain
C
Cumulative number of detected transcripts with effective SNPs
x10^4
allele 1
allele 2
CAST/129 RamDA-Seq
129/B6 C1/Smart-seq
CAST/B6 Smart-seq2
D
TBi noise = 0.9385
# of transcripts derived from Allele 2
# of transcripts derived from Allele 1
E
mean TBi noise
# of data points

Fig. S3

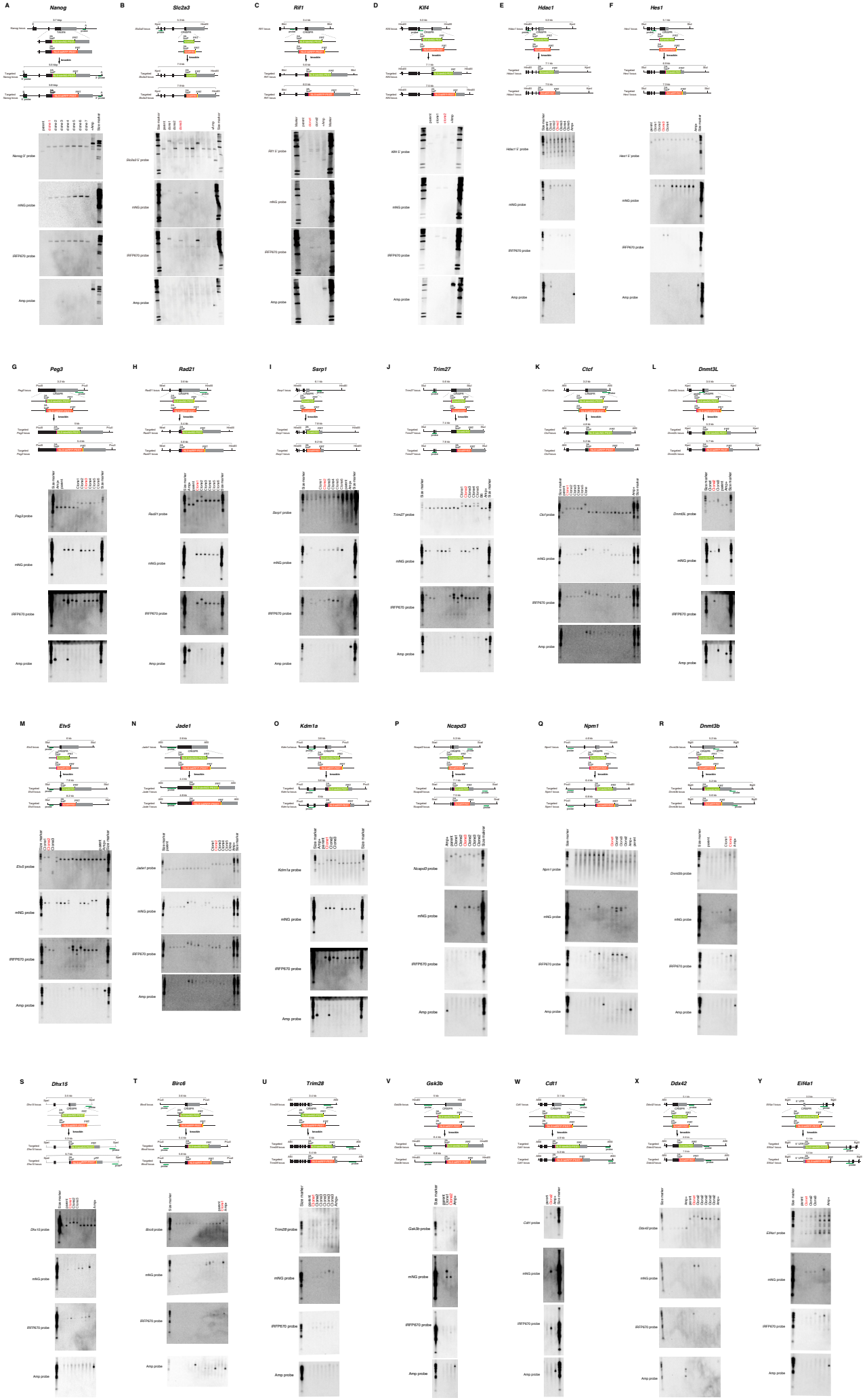
A
Nanog
B
Slc2a3
C
Rif1
D
Klf4
E
Hdac1
F
Hes1
G
Peg3
H
Rad21
I
Ssrp1
J
Trim27
K
Ctcf
L
Dnmt3L
M
Etv5
N
Jade1
O
Kdm1a
P
Ncapd3
Q
Npm1
R
Dnmt3b
S
Dhx15
T
Birc6
U
Trim28
V
Gsk3b
W
Cdt1
X
Ddx42
Y
Eif4a1
mNG probe
iRFP670 probe
Amp probe

Fig S4

A

	Length	Pvalue	Enrichment score	Number
High-motif-1	11	9.25E-173	-0.69	84
High-motif-2	11	9.85E-125	3.23	47
High-motif-3	10	2.33E-103	0.79	113
High-motif-4	10	3.11E-94	-1.02	107
High-motif-5	11	4.93E-84	0.44	121
Low-motif-1	12	3.32E-81	7.33	48
Low-motif-2	10	5.35E-81	1.21	45
Low-motif-3	11	6.82E-77	7.21	48
Low-motif-4	10	1.92E-76	5.85	79
Low-motif-5	12	8.77E-39	2.18	36

B

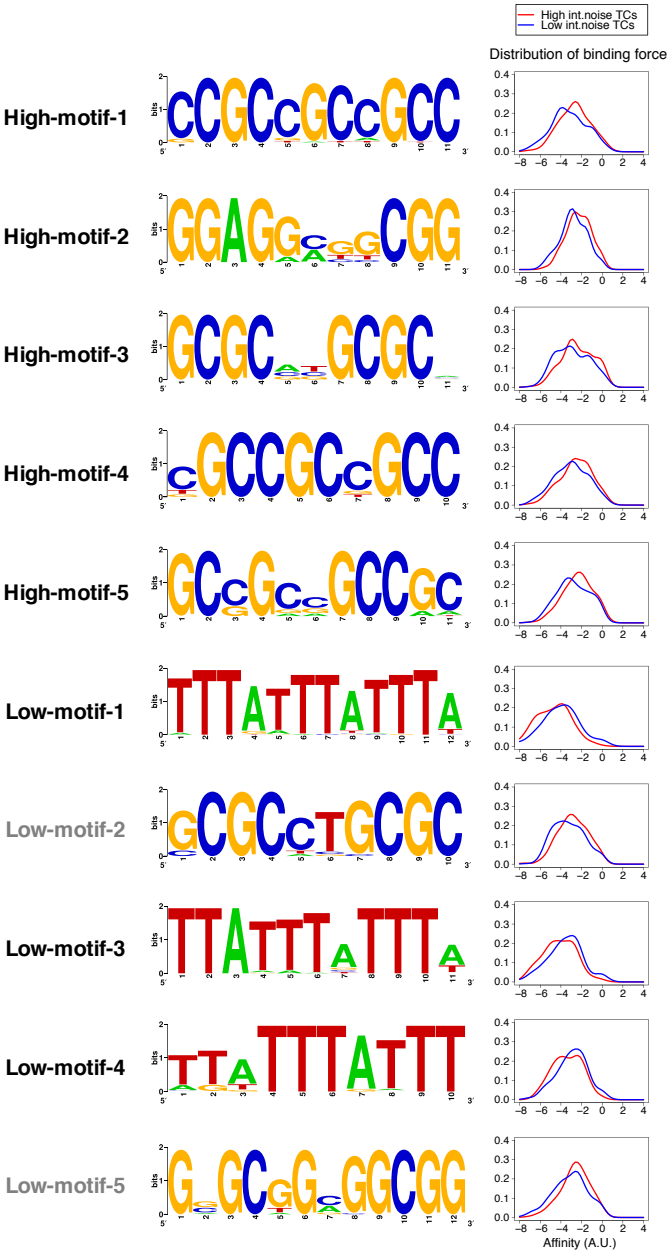

C

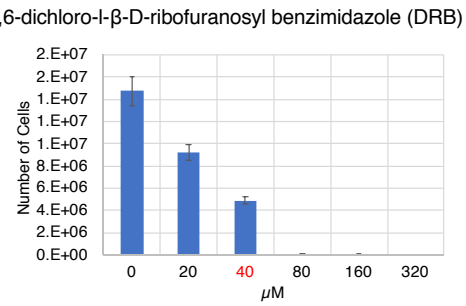

D

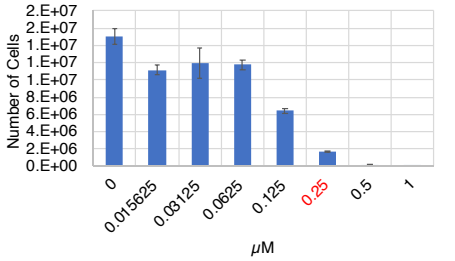

E

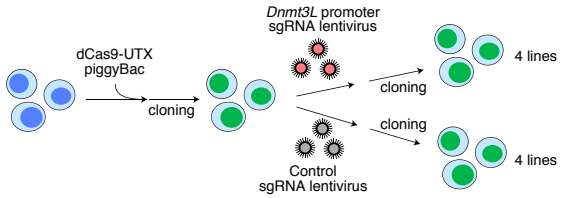

F

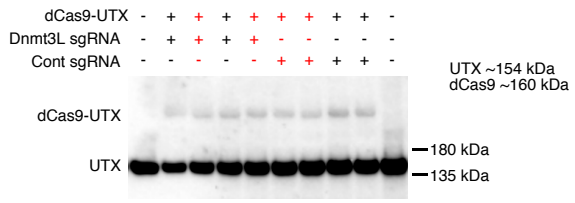

G

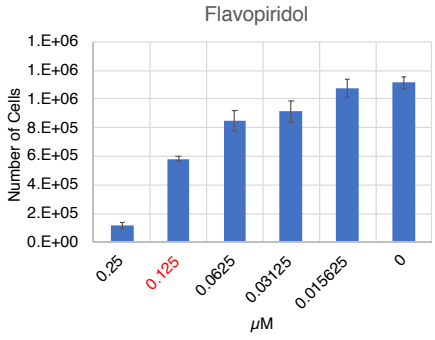

H

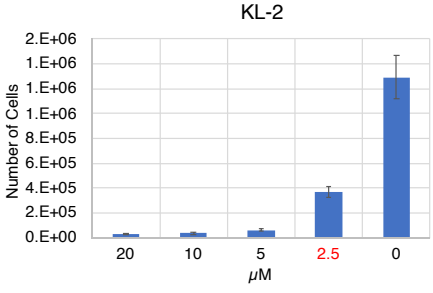

Fig. S5

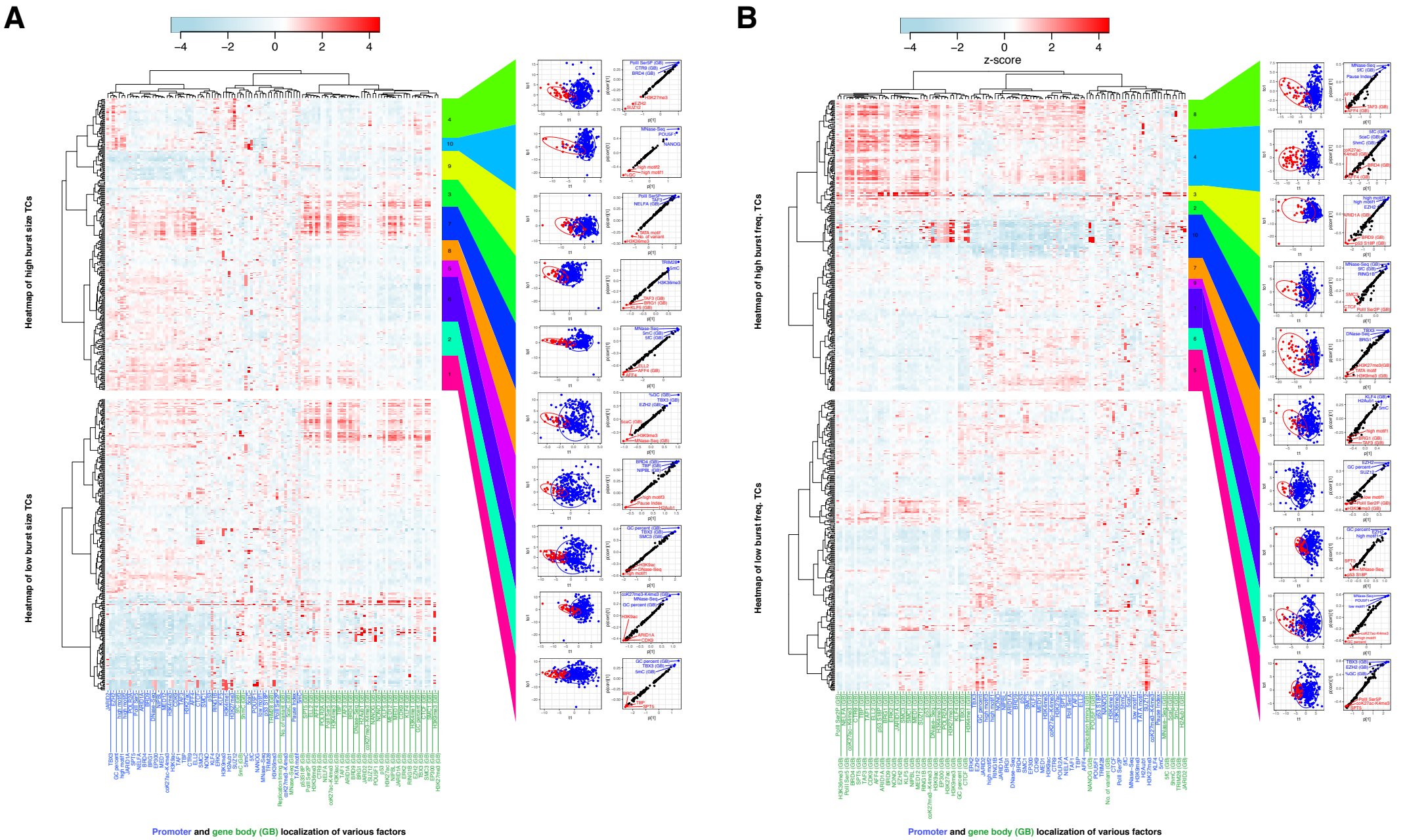
A
B
−4
−2
0
2
4
z-score
Heatmap of high burst size TCs
Heatmap of low burst size TCs
Heatmap of high burst freq. TCs
Heatmap of low burst freq. TCs
Promoter and gene body (GB) localization of various factors
Promoter and gene body (GB) localization of various factors

Fig. S6

A

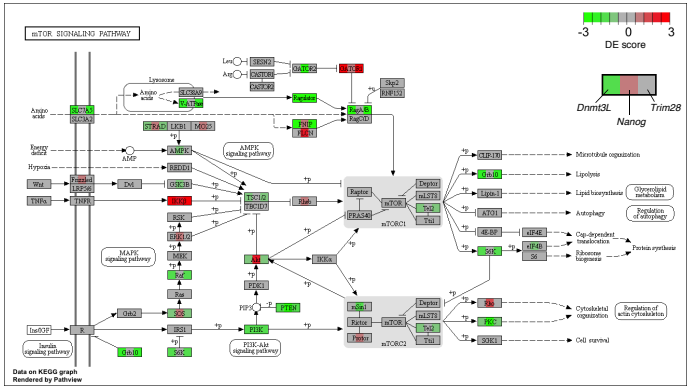
mTOR SIGNALING PATHWAY
DE score
-3 0 3
Dnmt3L Trim28
Nanog
Data on KEGG graph
Rendered by Pathview

B

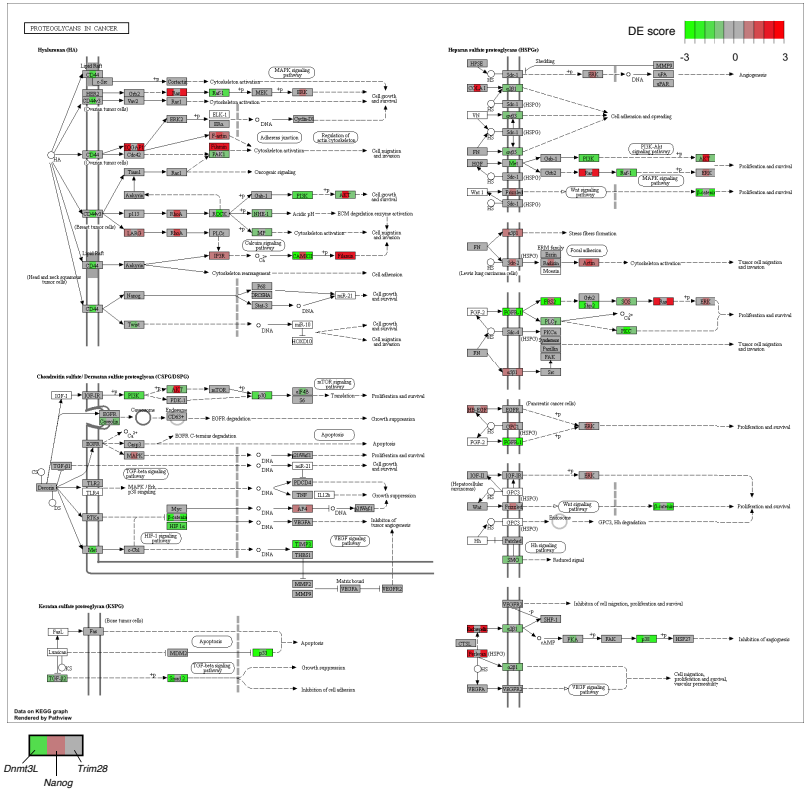
PROTEOGLYCANS IN CANCER
DE score
-3 0 3
Dnmt3L Trim28
Nanog
Data on KEGG graph
Rendered by Pathview

C

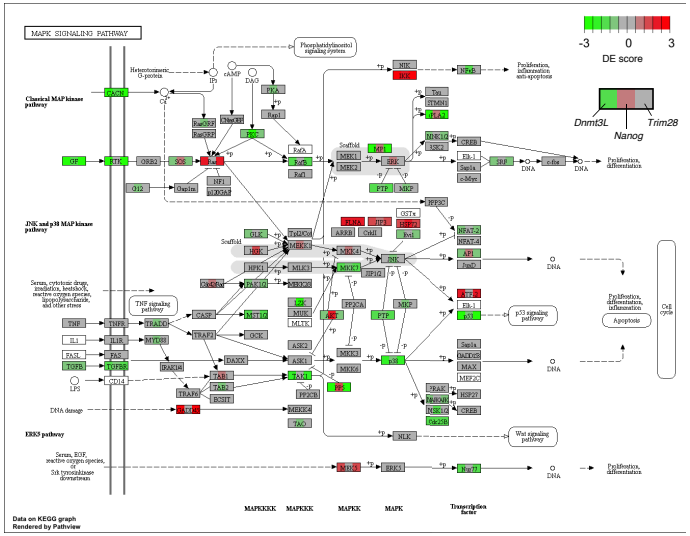
MAPK SIGNALING PATHWAY
DE score
-3 0 3
Dnmt3L Trim28
Nanog
Data on KEGG graph
Rendered by Pathview

D

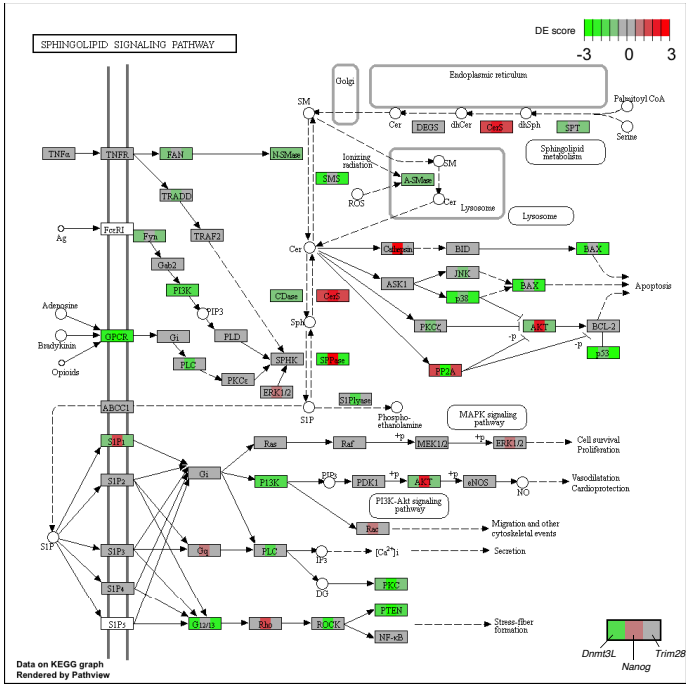
SPHINGOLIPID SIGNALING PATHWAY
DE score
-3 0 3
Dnmt3L Trim28
Nanog
Data on KEGG graph
Rendered by Pathview

Fig. S7

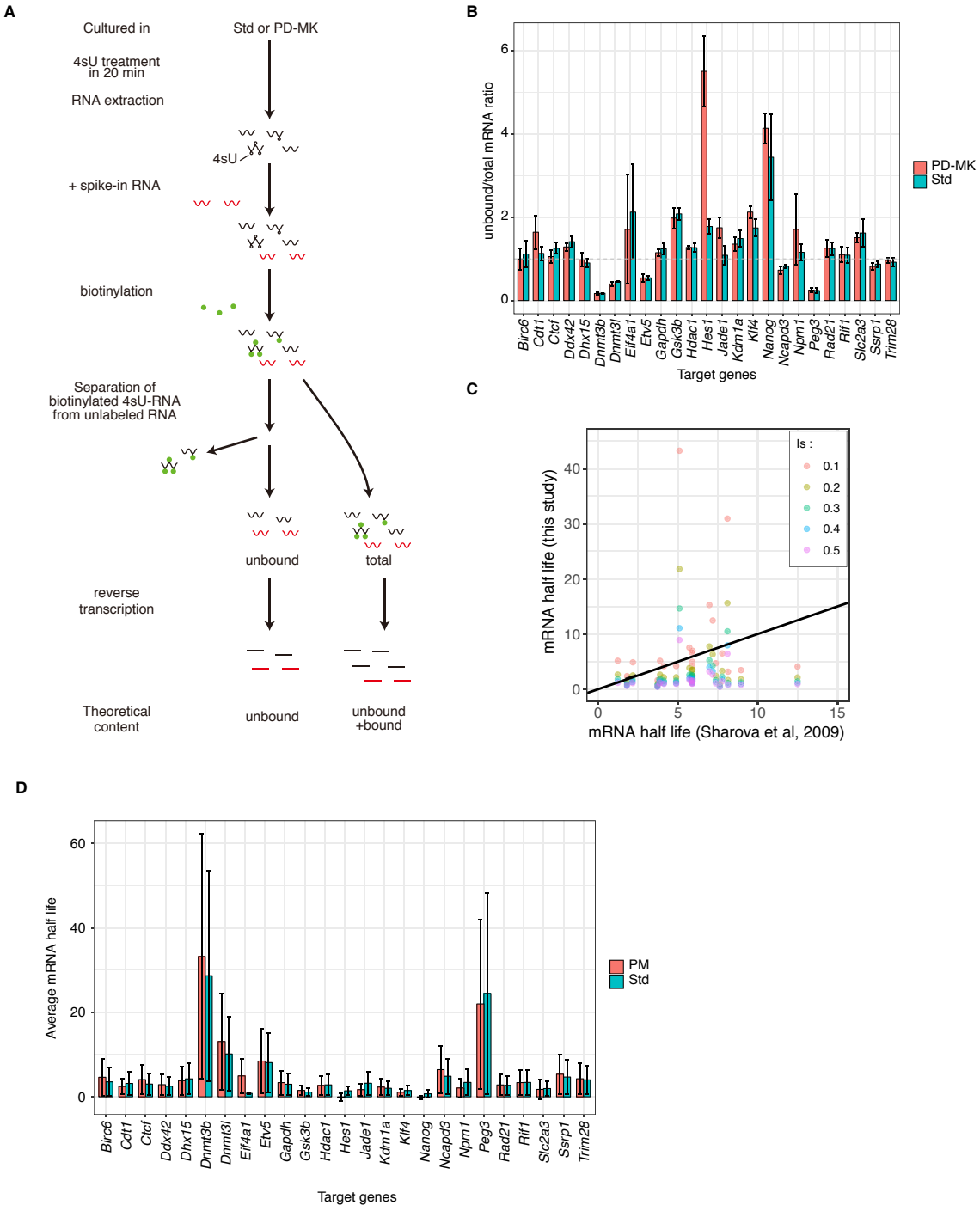
A
Cultured in
Std or PD-MK
4sU treatment in 20 min
RNA extraction
4sU
+ spike-in RNA
biotinylation
Separation of biotinylated 4sU-RNA from unlabeled RNA
unbound
total
reverse transcription
Theoretical content
unbound
unbound +bound
B
unbound/total mRNA ratio
PD-MK
Std
Birc6 Cdt1 Ctcf Ddx42 Dhx15 Dnmt3b Dnmt3l Eif4a1 Etv5 Gapdh Gsk3b Hdac1 Hes1 Jade1 Kdm1a Klf4 Nanog Ncapd3 Npm1 Peg3 Rad21 Rif1 Slc2a3 Ssrp1 Trim28
Target genes
C
mRNA half life (this study)
ls :
0.1
0.2
0.3
0.4
0.5
mRNA half life (Sharova et al, 2009)
D
Average mRNA half life
PM
Std
Birc6 Cdt1 Ctcf Ddx42 Dhx15 Dnmt3b Dnmt3l Eif4a1 Etv5 Gapdh Gsk3b Hdac1 Hes1 Jade1 Kdm1a Klf4 Nanog Ncapd3 Npm1 Peg3 Rad21 Rif1 Slc2a3 Ssrp1 Trim28
Target genes

Supplemental Information titles and legends.

Figure S1. Related to Figure 1. (A) The difference between the transcriptomes of mESCs cultured on either Laminin-511 or gelatin coated dishes was relatively subtle. mESCs were conditioned on either gelatin or Laminin-511 (LN 511) coated dish under either Std or 2i medium. RNA was extracted from these cells and analyzed by RNA-Seq. Two biological replicates were prepared. The result of clustering transcriptome data is shown. Biological replicates are similar to each other. The clusters are mainly divided into two clades depending on different medium conditions, suggesting that the influence of coating reagent difference (gelatin vs LN511) on the transcriptome is much smaller than that of the culture medium difference (Std vs 2i). (B-G) Processing of data obtained from scRNA-seq. (B) In order to calculate TBi noise, it was necessary to normalize so as to match the average expression level among alleles. Therefore, we first normalized the global expression level between alleles. Here, a scatter plot of the relationship between the mean read counts and total noise before and after a global normalization is shown. Even with global normalization, the shape of the distribution was not substantially changed. (C) Scatter plot of mean normalized read counts and TBi noise in data with expression levels that were normalized between alleles. Theoretically, TBi noise should not be less than Poisson noise (1 / mean read counts). Since data below the Poisson noise had a possibility of analytical defects, they were removed in subsequent analyses. TBi noise tends to decrease depending on the expression level. (D) Scatter plot of read count-normalized TBi noise and mean normalized read counts. (E) Scatter plot of count-normalized TBi noise and transcript length. (F) Scatter plot of count and transcript length-normalized TBi noise (referred as just normalized TBi noise) and transcript length. (G) Scatter plot of mRNA half-life and normalized TBi noise. There was no correlation between them (r = 0.0104). (H-I) Normalized TBi noise at mRNA level and protein level in KI cell line. To determine the normalized TBi noise at the mRNA and protein levels in the KI cell line, analysis was carried out with smFISH using allele specific probes (H) and flow cytometry (I) in these cell lines. Scatter plots of average expression level and TBi noise with regression lines are shown. The residuals from the regression line in the Y-axis direction were taken as normalized TBi noise. (J-K) Immunofluorescence of endogenous proteins in KI cell line. In some of KI cell lines, the protein expressed from the target gene was fluorescently immunostained, and the fluorescence image of the immunofluorescence together with GFP or iRFP derived from the knocked-in cassette was obtained by fluorescence microscopy. In addition, correlations of fluorescent intensity of

individual cells were examined. Since the KI cassette contains 2A peptide, nuclear localization signal (NLS)-GFP (or iRFP), and PEST sequence, which induces rapid protein degradation, these endogenous proteins and knocked-in fluorescent proteins become different protein molecules after translation. (J) Fluorescent images of fluorescent proteins and immunostained endogenous TRIM28 proteins in the *Trim28* KI cell line. The images show maximum intensity projections of stacks. The lower right panel shows a scatter plot of the fluorescence intensities of the fluorescent proteins and the fluorescent immunostaining. (K) A bar graph of the Spearman's rank correlation coefficients between the fluorescence intensities of the fluorescent protein and the fluorescent immunostaining of the endogenous protein. All proteins analyzed here showed substantial correlation, suggesting that the fluorescence intensity of the fluorescent protein is indicative of endogenous protein abundance.

Figure S2. Related to Figure 1. Comparison of the classification efficiency of each allele using SNPs with results of single-cell (sc) RNA-seq (RamDA-seq) with that of other studies. (A) Mean read coverage over transcripts of three datasets. "RamDA-seq, this study": CAST/129 mESC scRamDA-seq; "Kolodziejczyk et al., 2015": 129/B6 mESC C1/Smart-seq performed in [44]; "Larsson et al., 2019": CAST/B6 mESC Smart-seq2 performed in [37]. (B) The theoretical numbers of transcripts with effective SNPs in three different hybrid mESC genomes. (C) The cumulative number of detected transcripts with effective SNPs in three different experiments. CAST/129 RamDA-seq: CAST/129 mESC scRamDA-seq in this study; 129/B6 C1/Smart-seq: 129/B6 mESC C1/Smart-seq performed in [44]; CAST/B6 Smart-seq2: CAST/B6 mESC Smart-seq2 performed in [37]. The classification efficiency of each allele using the SNPs of this study was comparable to that of the other studies. (D, E) The number of samples affect the confidence of calculated TBi noise. (D) Each of the 1000 simulated datasets with 500 data points of the set of allele expression was generated. Mean expression of each allele and TBi noise in these data sets were 113.22 ± 5.74 (SD) and 0.958 ± 0.0799 (SD), respectively. One representative plot is shown. (E) Differences in standard deviation between datasets with different numbers of data points. We calculated the mean and standard deviation of TBi noise in datasets with different numbers of data points. Error bars indicate standard deviation. It is evident that the larger the number of data points, the smaller the data variation. We used 447 of 129/CAST mESCs in the G1 phase for the analysis of TBi noise in this study, while, Kumar et al., Kolodziejczyk et al., and Larsson et al. used 183 of 129/B6 mESCs, 250 of 129/B6 mESCs, and 188 of B6/CAST mESCs that were in different phases of the cell cycle and were cultured in Std medium or

unknown condition in their scRNA-seq, respectively [37,44,55]. Thus, our data are expected to be an important resource for a deeper understanding of transcriptional bursting and TBi noise.

Figure S3. Related to Figure 1. Establishment of knock-in cell lines. The upper part of the panel shows structures of the target gene near the knock-in site, the targeting vector, and the knocked-in genes. The results of Southern blotting are shown at the bottom of the panel. Parent means the parental strain (C57BL6J, Bruce4), +Amp means a cell line in which the ampicillin resistance gene, which is contained in the backbone of the targeting vector, has been introduced into the genome. Cell lines shown in red letters were used in the downstream experiments. See Table S6 for details of knock-in cell lines used in this study.

Figure S4. Related to Figure 2. (A-B) Motifs found in high and low TBi noise promoters. (A) The promoter regions (-500 to +100 from TSS) of high and low TBi noise transcripts (TCs) were analyzed using DMINDA [75] and characteristic motifs were searched. The sequences near the TSS of the 5992 TC whose average expression level was over 20 read counts were used as controls. Here we show the information in the top five motifs found in promoters of high or low TBi noise TCs. (B) The sequence LOGO of the motifs identified from the DMINDA analysis and the distribution of the binding force of these motifs to the high or low TBi noise TC promoter region (see Methods). Low-motif-2 and -5 were excluded from the subsequent analysis because the binding affinities were higher in the high TBi noise TCs. Also, since the sequences of High-motif-1, 4 and 5 are very similar, High-motif-4, 5 was excluded from subsequent analysis. Also, for Low-motif-1, 3, and 4 for the same reason, Low-motif-3 and 4 were excluded from subsequent analysis. (C-D) Effects of transcription elongation inhibitor on cell growth. 1×10^5 C57BL6J WT mESCs conditioned to 2i medium were cultured for 2 days in the presence of 5,6-dichloro-l-β-D-ribofuranosyl benzimidazole (DRB) (C) or Flavopiridol (D), and the number of cells were counted. We decided to use the concentration (highlighted in red letters), at which the growth rate drops sufficiently, and cells were not extinct, in the following experiment. (E-F) Establishment of cell lines used for epigenome editing. (E) Using *Dnmt3l* KI cells as the parent cell line, a cell line stably expressing dCas9-UTX was established. Then, using this cell line as a parent cell line, two types of cell lines stably expressing either sgRNAs for *Dnmt3l* promoter or control were established. Here, the schematic diagram is shown. See Methods for details. (F) Confirmation of the expression of dCas9-UTX in established cell lines done by western blot. We used clones highlighted in red in the downstream experiments. (G-H)

Effects of transcription elongation inhibitor on cell growth in mESCs conditioned PD-MK medium. 1×10^5 WT mESCs conditioned to PD-MK medium were cultured for 2 days in the presence of Flavopiridol (G) or SEC inhibitor KL-2 (H), and the number of cells were counted. We decided to use the concentration (highlighted in red letters), at which the growth rate drops sufficiently and cells were not extinct, in the following experiment.

Figure S5. Related to Figure 3. (A) Burst size is determined by combinations of promoter and gene body associating factors. First, the target 5992 transcripts (TCs) were ranked with the burst size, of which the upper or lower 5% (300 TCs each) was taken as high and low burst size TCs, respectively. The left side of the panel shows a heat map of promoter and gene body (GB) association of various factors in high and low burst size TCs. The high burst size TCs were classified into 10 clusters, and each cluster of high burst size TCs and whole low burst size TCs were subjected to OPLS-DA modeling. The right side of the panel represent score plots of OPLS-DA and S-plots constructed by presenting covariance (*p*) against correlation [*p*(*corr*)]. (B) Burst frequency is determined by combinations of promoter and gene body associating factors. First, the target 5992 transcripts (TCs) were ranked with the burst frequency, of which the upper or lower 5% (300 TCs each) was taken as high and low burst frequency TCs, respectively. The left side of the panel shows a heat map of promoter and gene body (GB) association of various factors in high and low burst frequency TCs. The high burst frequency TCs were classified into 10 clusters, and each cluster of high burst frequency TCs and whole low burst frequency TCs were subjected to OPLS-DA modeling. The right side of the panel represents score plots of OPLS-DA and S-plots constructed by presenting covariance (*p*) against correlation [*p*(*corr*)].

Figure S6. Related to Figure 4. KEGG pathways of negatively-enriched genes in three independent CRISPR library screens. The color within each gene shows the DE score. The color on the left, middle, and right side in each gene mean DE score obtained by screening of *Dnmt3l*, *Nanog*, and *Trim28* KI cell lines, respectively.

Figure S7. Related to Figure 4. RNA degradation rate between PD-MK and Std conditions did not show significant difference. (A) Schematic representation of the experiment for examining RNA degradation rate. WT mESCs were transiently treated with 4-thiouridine (4sU). By this transient treatment, 4sUs were incorporated into newly synthesized RNA. RNA was then

extracted from the cells, and a known amount of spike-in RNA that does not contain 4sU was added. Thereafter, the RNA mix was biotinylated. Then, from a part of this biotinylated RNA mix, biotinylated RNA was removed using streptavidin beads, and unbiotinylated RNAs that were transcribed before the addition of 4sU were recovered. RNA samples that were not treated with streptavidin beads contained both existing RNA and newly synthesized RNA. Therefore, we refer to these RNA samples as total RNAs. These were reverse transcribed and analyzed by qPCR. (B) A bar graph of the ratio of unbound and total RNA. For many samples, the ratio has exceeded 1, which was theoretically impossible. It is considered that the reverse transcription efficiency of 4sU-introduced RNA could be extremely low (see Methods). (C) We assumed that the presence of biotinylated RNA during reverse transcription may trap the reverse transcriptase, and that the efficiency of reverse transcription is further globally reduced. We assume that the global suppression effect of reverse transcriptase trapping is I_g (global inhibitory effect). Moreover, the reverse transcription inhibitory effect of biotinylated RNA itself was defined as I_s (see Methods). In order to determine the appropriate value of I_s, several values were assigned to I_s, and mRNA half-lives in the Std condition were compared with the previously reported mRNA half-lives [32]. We found that scaling of mRNA half-lives in the Std condition and that of previously reported mRNA half-lives were getting closer when I_s was 0.1. (D) Average mRNA half-life. The half-life of mRNA was calculated using the ratio obtained in (B) and the correction formula (see Methods). In all genes analyzed, there was no significant difference between PD-MK and Std conditions.

Supplemental item titles and legends

Table S1. Allelically normalized read count data of individual transcripts of 129 alleles. Related to Fig. 1. Data with TBi noise below Poisson noise or transcripts showing interallelic extreme expression level differences are removed (see Methods).

Table S2. Allelically normalized read count data of individual transcripts of CAST alleles. Related to Fig. 1. Data with TBi noise below Poisson noise or transcripts showing interallelic extreme expression level differences are removed (see Methods).

Table S3. Allelically normalized read count data of individual genes of 129 alleles. Related to Fig. 1 and S1. Data with TBi noise below Poisson noise are removed (see Methods).

Table S4. Allelically normalized read count data of individual genes of CAST alleles. Related to Fig. 1 and S1. Data with TBi noise below Poisson noise are removed (see Methods).

Table S5. smFISH count data of GFP and iRFP knocked-in allele in knock-in cell line. Related to Fig. 1 and S1.

Table S6. Plasmids information used for knock-in cell line establishment and sequences of oligos used in this study. Related to Fig. 1, 2, 4 and S1, S3, S4, S7.

Table S7. List of data sources used in this study. Related to Fig. 3 and S5.